Dependence of Magnetoresistance in Electrodeposited CoNiCu/Cu Multilayers on Ni Composition

Article *in* ECS Transactions · January 2010

DOI: 10.1149/1.3422502

CITATIONS
2

READS
26

3 authors, including:

Mursel Alper
Uludag University
109 PUBLICATIONS **1,044** CITATIONS
SEE PROFILE

Hakan Köçkar
Balikesir University
177 PUBLICATIONS **977** CITATIONS
SEE PROFILE

Journal of The Electrochemical Society, **157** (10) D538-D545 (2010)
0013-4651/2010/157(10)/D538/8/$28.00 © The Electrochemical Society

Magnetoresistance of CoNiCu/Cu Multilayers Electrodeposited from Electrolytes with Different Ni Ion Concentrations

M. Safak Haciismailoglu,[a,*] M. Alper,[a,z] and H. Kockar[b]

[a]*Department of Physics, Faculty of Science and Literature, University of Uludag, Görükle, Bursa 16059, Turkey*
[b]*Department of Physics, Faculty of Science and Literature, University of Balıkesir, Balıkesir 10145, Turkey*

A series of CoNiCu/Cu multilayers was potentiostatically electrodeposited on strong (100) textured Cu substrates from electrolytes with different Ni concentrations. X-ray diffraction patterns showed that all studied samples exhibited a face-centered cubic structure. From scanning electron microscopy images, it was observed that the surface morphology of the films is affected by their Ni content. The compositional analysis by energy-dispersive X-ray spectroscopy demonstrated that as the Ni ion concentration in the electrolyte is increased, the Ni content of the film increases. Magnetoresistance (MR) measurements were carried out at room temperature in the magnetic fields of ± 12 kOe. The samples grown from the electrolytes with the Ni concentration of up to 0.3 M exhibited giant magnetoresistance (GMR). For the samples grown from 0.3 M Ni, anisotropic magnetoresistance (AMR) begins to appear as well as GMR. As the Ni concentration in the electrolytes is increased, the AMR effect enhances, whereas the GMR effect weakens. For the 2.0 M Ni concentration, the MR behavior of multilayers converts from GMR to AMR. Furthermore, the magnetization measurements made by a vibrating sample magnetometer showed that the antiferromagnetic coupling between ferromagnetic layers weakens with increasing the Ni concentrations.
 [DOI: 10.1149/1.3469583]

Manuscript submitted May 25, 2010; revised manuscript received July 2, 2010. Published August 19, 2010.

Nanostructured ferromagnetic materials such as conventional and nanowired multilayers have attracted much attention due to their interesting properties such as giant magnetoresistance (GMR) effect and spintronic applications. Electrodeposition is one of the highly versatile techniques to produce such nanostructured metallic materials and has many advantages such as low cost, easy scale-up, and rapid deposition at room temperature and pressure. Although electrodeposited magnetic multilayers have smaller GMR values compared to those of multilayers grown by vacuum-based processes such as sputtering,[1-3] it can be possible to improve the GMR values in the electrodeposition process because the GMR can be affected by many chemical parameters such as the electrolyte concentration, the electrolyte pH, and the deposition potential as well as physical parameters such as the layer thickness, bilayer number, and substrate.[4-8]

As in vacuum processes, electrodeposition cannot provide pure ferromagnetic layers but rather a ferromagnetic metal-rich alloy layer, like a Ni-rich NiCu alloy in the Ni/Cu multilayers or a Co-rich CoCu alloy in Co/Cu multilayers. Particularly, in electrodeposited multilayers based on Co and Cu, at the interface between Co and Cu sublayers, the anodic dissolution of Co can occur during the deposition of a more noble metal Cu, which results in a highly Cu-rich region adjacent to the Co sublayer and fluctuation interfaces. This event decreases the GMR of the electrodeposited CoCu/Cu multilayers. Using some additives and adjusting electrolyte concentrations, few works have been done to improve the CoCu/Cu multilayer structure[9,10] by inhibiting the displacement of Co by Cu. For example, the addition of Ni to the Co layer has been reported to raise the GMR value but when the multilayers were electrodeposited at low pH (2.0).[11,12]

In this study, structural, chemical, magnetoresistance (MR), and magnetic properties of CoNiCu/Cu multilayers were studied as a function of Ni concentration in the electrolyte and hence the Ni content in the film. Structural, magnetic, and MR characterizations of the films are significantly affected by Ni concentration in the electrolyte. A small Ni component concentration of CoNiCu/Cu multilayers was found to enhance the GMR effect, which is thought to arise from a lowering of the displacement reaction. More Ni addition reduces the GMR, in which rather than the displacement reaction, the electrolyte pH plays a more effective role on the GMR because the low electrolyte pH (2.0) is known to increase the GMR of CoNiCu/Cu multilayers.[11]

Experimental

Polycrystalline Cu sheets, having a strong (100) texture of the face-centered cubic (fcc) structure, were used as substrate. Before deposition, one face of each substrate was polished mechanically using emery papers with different grades and then covered with an electroplating tape except for a circular area ~ 3 cm^2 of the polished face. The uncovered area, which was exposed to the electrolyte, was electropolished in 50 vol % H_3PO_4 solution until a bright face was obtained. After polishing, the substrate was in turn rinsed in 25 vol % H_3PO_4, 10 vol % H_3PO_4, distilled water, 10 vol % H_2SO_4, and finally distilled water. The polished sample was immediately placed into the electrolyte used to deposit multilayers. For CoCu/Cu multilayers, an electrolyte composed of 0.27 mol/L cobalt sulfate (from $CoSO_4 \cdot 7H_2O$), 0.022 mol/L copper sulfate (from $CuSO_4 \cdot 5H_2O$), 0.022 mol/L boric acid (H_3BO_3), and 0.01 mol/L sulfamic acid (NH_2SO_3H) was used. To study the effect of Ni, a series of electrolyte was prepared by adding nickel sulfamate [$Ni(SO_3NH_2)_2 4H_2O$] with different concentrations (0–2.0 mol/L) to the electrolyte used to grow CoCu/Cu multilayers. CoNiCu/Cu multilayers were grown from these electrolytes. The pH value for all electrolytes was 2.5 ± 0.1. Deposition was carried out in a three-electrode cell with the use of an EG&G model 362 controlled by a personal computer and without any agitation. A platinum (Pt) sheet was used as counter electrode (anode) and a saturated calomel electrode (SCE) served as the reference electrode. The deposition of Cu layers was made at a cathode potential of -0.4 V with respect to SCE, whereas the ferromagnetic Co and CoNi layers were deposited at -1.5 V vs SCE. The nominal thicknesses of Co (or CoNi) and Cu sublayers were fixed at 4 and 0.7 nm, respectively, assuming 100% current efficiency. The bilayer number was chosen to be 426 to keep constant the total thickness of samples at 2 μm, that is, the multilayers had a form of 426[CoNiCu (4 nm)/Cu (0.7 nm)]. During each pulse, a fixed amount of charge was passed to obtain a ferromagnetic or nonmagnetic layer of the desired thickness. Because the thickness of the Cu layer in all multilayers was the same and Cu was deposited at a limiting current, no change in the composition of the Cu layer is expected with the variation in the deposition parameters. Therefore, any variation in the film composition would occur only in the ferromagnetic layer. The current transient was recorded and analyzed to obtain information about the dissolution of the ferromag-

* Electrochemical Society Student Member.
z E-mail: malper@uludag.edu.tr

netic layers occurring during the deposition of Cu. After growth, all samples, except for the vibrating sample magnetometer (VSM) samples, were peeled off their substrates electrochemically.

The structural analysis of the films was made using X-ray diffraction (XRD) with Cu Kα radiation (λ = 0.15406 nm). The diffraction patterns were obtained in the range of 2θ = 40–100° with a step of Δ(2θ) = 0.02° because the main Bragg reflections of bulk Cu in the fcc structure are between 2θ = 40 and 100°. Grain sizes for each reflection were calculated using the Scherrer formula[13]

$$t = \frac{0.9\lambda}{B \cos \theta_B} \quad [1]$$

where θ is the Bragg diffraction angle and B is the width of the peak at half-maximum intensity. The average grain size for a sample was calculated by taking into account the grain size and the texture coefficient for all reflections in its XRD pattern.[14] A scanning electron microscope (SEM, Zeiss 50 VP) attached with an energy-dispersive X-ray spectroscope (EDX, Oxford Instruments Inca Energy) was used for morphological observations and to determine the microstructural composition of the films. MR measurements were made at room temperature in the magnetic fields of ±12 kOe using the van der Pauw (VDP) method with four probes on the corners of a square sample. The magnetic field was applied both parallel and perpendicular to the current flowing through the film plane to measure longitudinal magnetoresistance (LMR) and transverse magnetoresistance (TMR), respectively. In each case, the percentage change in the resistance MR (%) as a function of the applied magnetic field was calculated according to the relation

$$\text{MR } (\%) = \frac{R(H) - R_{\min}}{R_{\min}} \times 100 \quad [2]$$

where $R(H)$ is the value of resistance at any magnetic field (H) and $R_{\min}$ is the value at the field where the resistance is minimum. Interlayer exchange coupling constant (J) was calculated according to Eq. 3

$$H_s = -\frac{4J}{M_s t_{FM}} \quad [3]$$

where H_s is the saturation magnetic field at which magnetization reaches 0.95 M_S, M_S is the saturation magnetization, and t_{FM} is the ferromagnetic layer thickness. The magnetic properties of the multilayers were studied by VSM, and from the obtained hysteresis curves, the saturation magnetization (M_s), the remanent magnetization (M_r), the coercivity (H_c), and the remanence ratio ($S = M_r/M_s$) were calculated.

Results and Discussion

Electrochemical characterization.— Figure 1 shows current–time transients for the first few layers of a CoNi/Cu multilayer grown from the electrolyte including 0.02 M Ni. On the cathodic side, the high current density pulses correspond to the CoNi layers and the low current density to the Cu layers. The deposition time for Cu layers is longer than that for CoNi layers because the total concentration of Co and Ni ions is more than the Cu ion concentration and, also, the deposition potential of the CoNi layers is higher than that of Cu layers. As seen from Fig. 1 for each Cu layer, the deposition current changes with time from positive to a stable negative value, and its deposition time lasts longer than that of the previous layer because the Cu concentration close to the surface of the cathode decreases with time. The high cathodic current occurring at the onset of the deposition of CoNi layers is probably due to the double layer charging current between the cathode and the solution. The anodic peak appeared at the beginning of the deposition of each Cu layer arises from the Co dissolution and the exchange reaction between Co and Cu. After the instantaneous transients, the current density for both the CoNi and Cu layers is almost constant. This suggests that both the CoNi and Cu layers were grown in a stable current. Similar current density transients were observed for other studied samples as well.

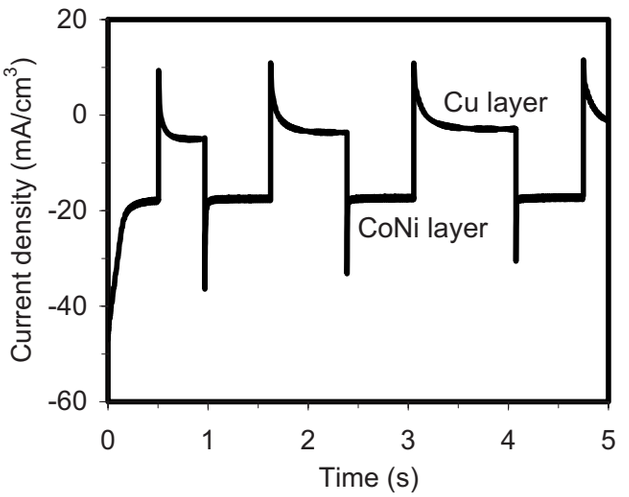

Figure 1. Current density transients of a CoNi/Cu multilayer grown from the electrolyte including 0.02 M Ni.

Structural analysis.— Figure 2 shows the typical XRD patterns of CoNiCu/Cu multilayers grown from electrolytes having different Ni ion concentrations, from 0.0 to 2.0 M. The structural analysis showed that all samples have a polycrystalline fcc structure. As seen from Fig. 2, for the CoCu/Cu (without Ni) and CoNiCu/Cu multilayers with 0.02 and 0.05 M Ni, the main Bragg peaks of the fcc structure are clearly seen at 2θ ≈ 43, 51, 75, and 91°, which correspond to the mean lattice spacings of the whole multilayer stack for the (111), (200), (311), and (220) reflections, respectively. For

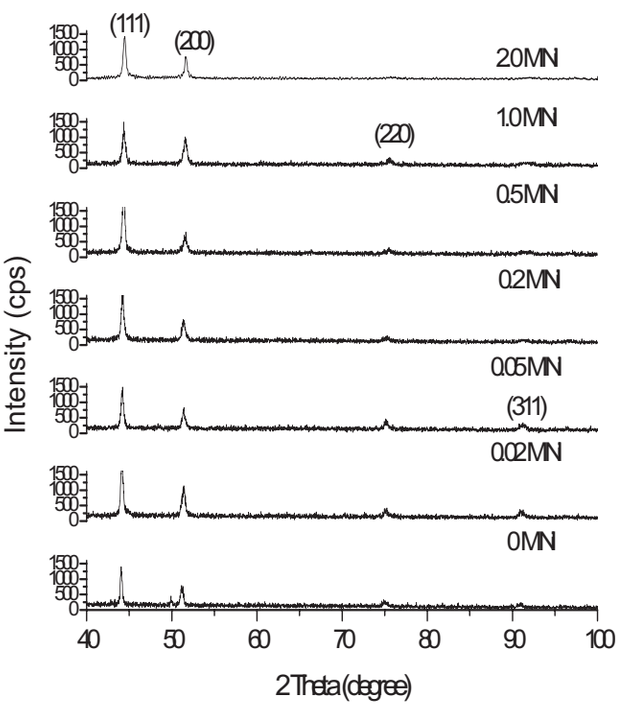

Figure 2. XRD patterns of multilayers with 426[CoNiCu (4 nm)/Cu (0.7 nm)] grown from the electrolytes with different Ni concentrations.

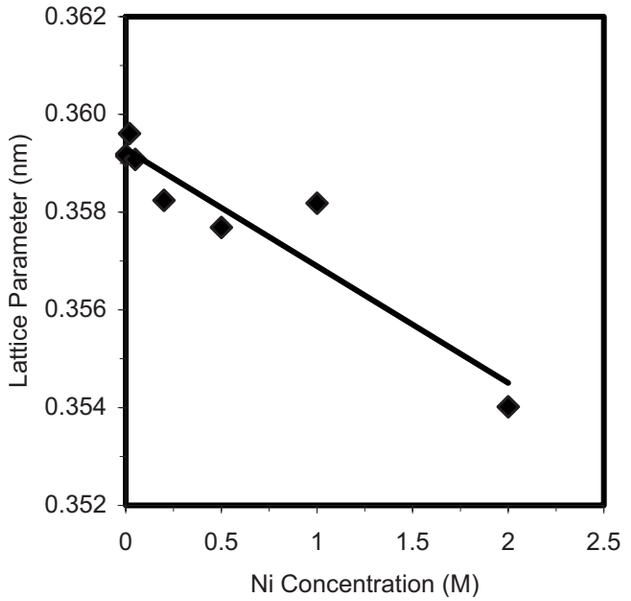

Figure 3. Variation in the lattices parameter of CoNiCu/Cu multilayers with the Ni concentration in the electrolyte.

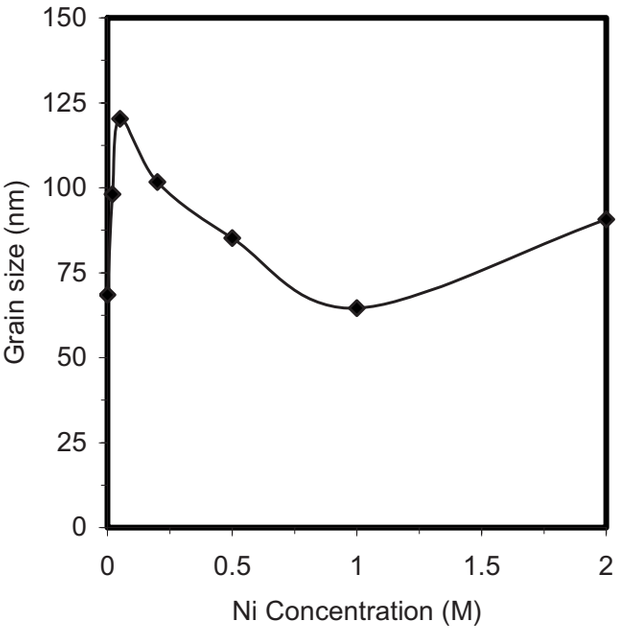

Figure 4. Variation in the average grain size of CoNiCu/Cu multilayers with the Ni concentration in the electrolyte.

samples with 0.2, 0.5, and 1.0 M Ni, the (311) reflection was not detected, and for the sample with 2.0 M Ni, both the (311) and (220) reflections were not detected. The preferential orientation of the samples was determined by calculating their texture coefficients from the experimental and theoretical relative integral intensities of the (*hkl*) reflections.[14] According to these findings, most of the multilayers have the same texture as in their substrates except for a few samples, indicating that the Cu substrate induces the growth of the multilayers in the (100) direction. However, the strength of the preferred orientation varies depending on the Ni ion concentration in the electrolyte and hence the Ni content of the deposit. As the Ni ion concentration increases, the orientation of the films can change as (111) or (100). The (111) orientation probably arises from the (111) preferred orientation of bulk Ni (or Cu), whereas it is (100) from the Cu substrate with strong (100) texture. No satellite peak was detected. This is probably due to the overlap of Co and Cu layers because the dissolution of Co prevents the formation of sharp interfaces. The absence of satellite lines is typical phenomena observed in electrodeposited multilayers with discontinuous interfaces.[15]

The lattice parameter of the samples was calculated using the least-squares technique by taking into account all reflections in the pattern. Figure 3 shows the variation in the lattice parameter of multilayers with Ni ion concentration in the electrolyte. Experimental data (solid squares) were fitted to a straight line. As expected, the lattice parameter of the samples decrease with increasing Ni concentration, that is, it shifts to that of the bulk Ni (a = 0.3524 nm). Lattice parameters are always intermediate between the values of the bulk Cu (0.3615 nm) and bulk Ni (0.3524 nm), indicating good coherency between the layers.

Figure 4 demonstrates the variation in the average grain size of the samples with respect to Ni ion concentration in the electrolytes, which may give about the structural coherence of the multilayers. For the low Ni concentrations ($<$0.05 M) (Fig. 5a), the average grain size increases as the Ni content in the film increases (Fig. 5b). Beyond this point, it continuously decreases, except for 2.0 M Ni (Fig. 5c). This suggests that the coherence of the multilayers becomes better until 0.05 M Ni concentration, and for higher Ni concentrations, it gets worse.[16,17] These results indicate that the addition of Ni less than 0.05 M improves the multilayer structure.

Figure 5 shows the SEM morphology of the CoNiCu/Cu multilayers deposited from the electrolytes with three different Ni concentrations. The pictures were taken from the solution side. The figure reflects the effect of Ni content on the surface morphology of the multilayer films. The film surface exhibits almost a uniform granular morphology for the low Ni concentration, but for the higher Ni concentration, some round islands occur.

Compositional analysis.— The composition of the multilayers was determined by EDX on at least three different areas for each sample. The average composition was calculated and the variation in the average composition within a sample was less than 5%, indicating compositionally a good uniformity. Figure 6 shows the variation in the average composition of the CoNiCu/Cu multilayers with Ni ion concentration. As seen from the figure, a continuous increase in the Ni content of the multilayers is observed with increasing Ni concentration, whereas the Co content decreases from ~68 to ~25%. This is an expected result because a fixed amount of metal is discharged at higher potentials (−1.5 V) to give the desired thickness of a ferromagnetic layer. The Cu content of the films decreases as the Ni concentration in the electrolyte increases. The Cu deposition is diffusion-limited; the amount of Cu deposited at the low potential pulse (−0.4 V) should be the same for all multilayers. Therefore, the higher Cu content in the films grown from the electrolytes without Ni and containing lower Ni concentrations indicates the presence of more Cu in the ferromagnetic layers. A possible explanation of this result is that Ni addition to the electrolytes containing Co and Cu ions reduces the dissolution of the ferromagnetic layer.

Figure 7 shows the Ni/Co ratio in the films as a function of the Ni/Co ratio in the electrolyte. As the Ni/Co ratio in the electrolyte increases, the Ni/Co ratio in the films increases linearly. The Ni/Co value in the films is almost half of that in the electrolyte. This proves that the anomalous codeposition occurs at each solution because in iron group metals, the deposition of a less noble metal is favored compared to that of a more noble metal.[18]

MR properties.— Four-probe MR measurements were used to investigate the GMR properties of the 426[CoNiCu (4 nm)/Cu (0.7 nm)] multilayers. The MR values (the percentage changes in the VDP resistance in the magnetic field) were calculated using Eq. 2. Figure 8 shows a characteristic evolution of the shapes of the MR curves with Ni concentration in the electrolyte. The solid lines rep-

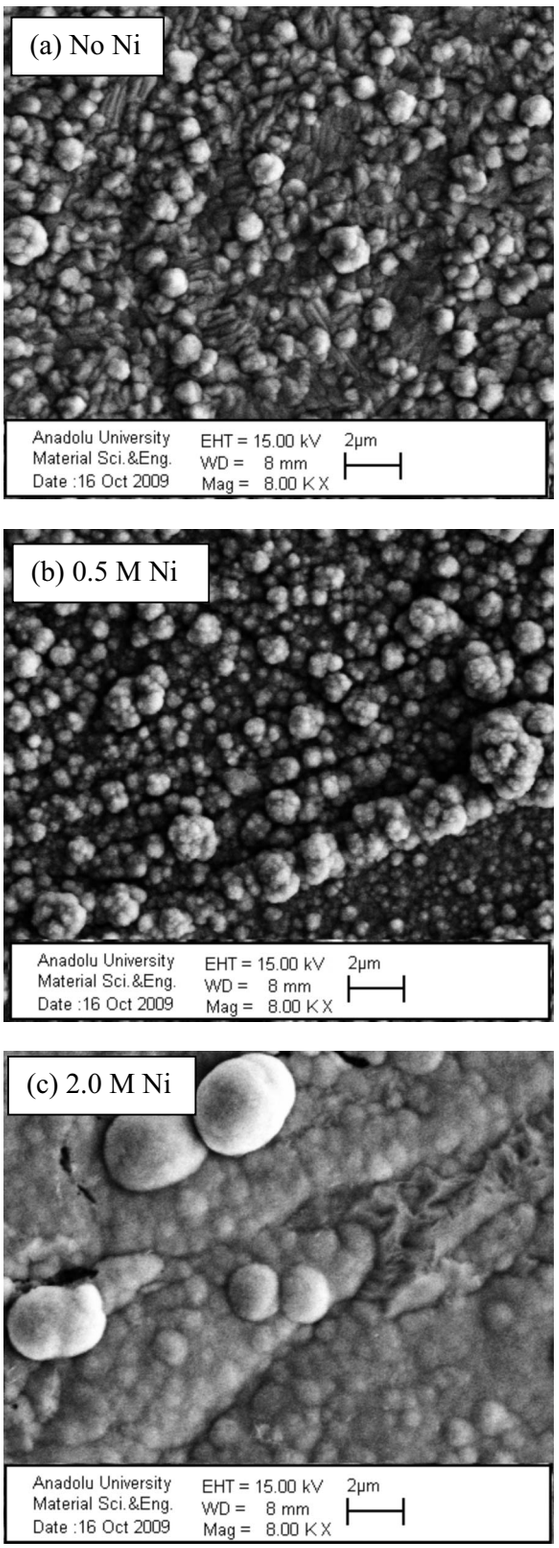

Figure 5. SEM images of multilayers with 426[CoNiCu (4 nm)/Cu (0.7 nm)] deposited from the electrolyte with different Ni concentrations.

resent the LMR and the circles indicate the TMR. As the magnetic field increases, both LMR and TMR decrease, i.e., the films exhibit the GMR effect arising from the periodicity of the multilayers. In Fig. 8, the addition of Ni up to 0.2 M to the CoCu/Cu multilayer

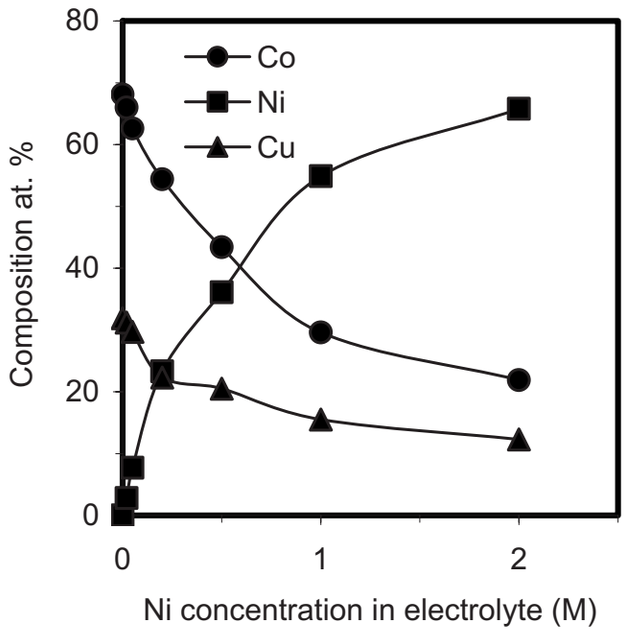

Figure 6. Composition of Co(Ni)Cu/Cu multilayers with the Ni concentration in the electrolyte.

systems enhances the GMR, that is, the CoNiCu/Cu multilayers exhibit a GMR larger than that in CoCu/Cu systems. This result can be explained by the fact that Ni addition improves the multilayer structure by suppressing the dissolution of Co.[19,20] The maximum value of the GMR is obtained for CoNiCu/Cu multilayers produced from the electrolyte containing 0.02 M Ni concentration. For the samples with over 0.2 M Ni, as the Ni concentration increases, the GMR decreases and, also, the anisotropic magnetoresistance (AMR) effect begins to appear. As seen in Fig. 8d, for the Ni concentration of 2.0 M, the TMR decreases and LMR increases with increasing magnetic field. The MR behavior of the film converts to almost the AMR

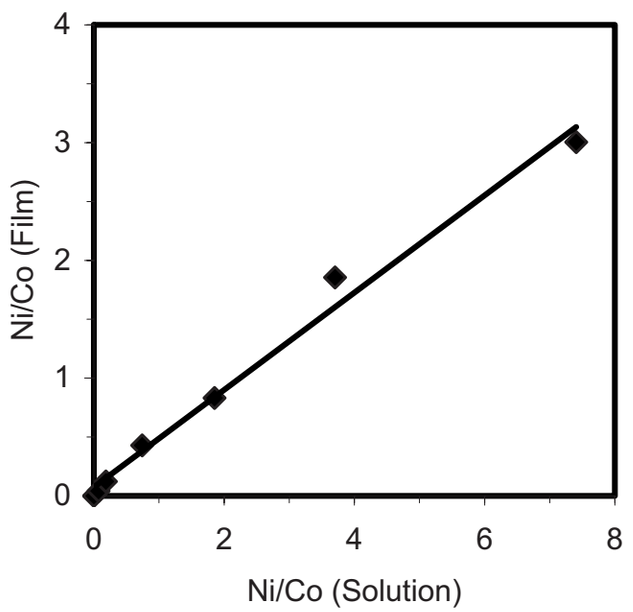

Figure 7. Variation in Ni/Co ratio in the films as a function of Ni/Co ratio in the solution.

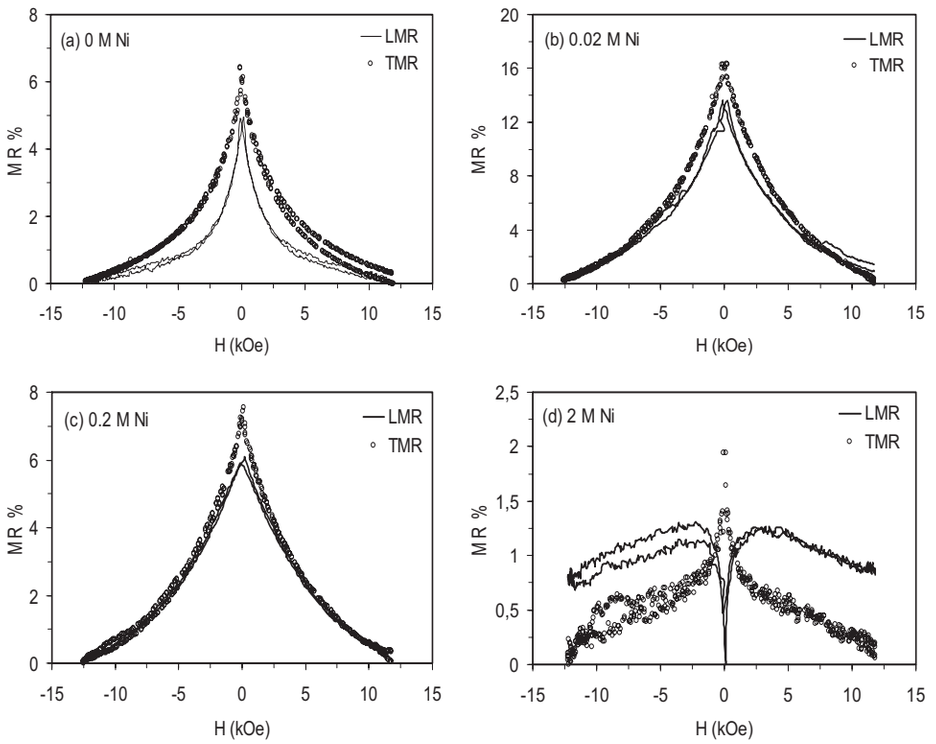

Figure 8. Development of GMR in multilayers with 426[CoNiCu (4 nm)/Cu (0.7 nm)] depending on the Ni concentration in the electrolyte.

effect, like bulk ferromagnetic alloys.[21] For high Ni concentrations, although increasing Ni concentration improves the multilayer structure, the diminish of the GMR effect may be a result of a high pH value of the electrolyte because in NiCoCu/Cu multilayers with high Ni concentrations, the GMR is strongly affected by the electrolyte pH.[11] Another point is that the Cu content decreases with increasing Ni concentration and as a result for this, the GMR weakens, as reported by Hua et al.[22,23]

To see clearly the behavior of the MR curves in small magnetic fields, the TMR curves of CoNiCu/Cu at the magnetic fields applied below 5 kOe are given in Fig. 9. All MR curves have the two peaks near the coercive field, corresponding to the antiparallel alignment of the magnetizations in adjacent ferromagnetic layers. These peaks corresponding to the maximum value of the resistivity shift to the small magnetic fields as the Ni concentration in the electrolyte and hence the Ni content in the sample increases. As seen later, this result was also confirmed by the hysteresis curves of the deposits.

The variation in GMR with Ni concentration in the electrolyte is given in Fig. 10. The inset in the figure shows the variation in GMR for Ni concentrations less than 0.3 M. As seen from the figures, the GMR of the CoNiCu/Cu multilayers with low Ni concentrations is larger than that of the multilayers with high Ni concentrations. The decrease in the GMR with increasing Ni concentration originates from the fact that the antiferromagnetic coupling between the Ni layers is weaker than the coupling between the Co layers. As seen later, this result was also confirmed by magnetization measurements. Furthermore, there are many studies that the GMR of Co/Cu multilayers have been reported to be larger than that of Ni/Cu.[24-27]

Interlayer exchange coupling constants (J) of the multilayers were calculated according to Eq. 3. For a CoNiCu/Cu multilayer grown from the electrolyte with 0.02 M Ni ion, which has the largest GMR value, J is 0.18 erg/cm^2. The $|J|$ value of Ni is smaller than Co or Fe.[28,29] The $|J|$ value of the CoNiCu/Cu multilayer grown from the electrolyte containing 0.02 M Ni is close to that of Co/Cu multilayers. The Co amount in the ferromagnetic layers is larger than the Ni content. Moreover, the GMR of the multilayers almost coherently varies with the average grain size. The increase in GMR with the grain size was attributed to many antiferromagnetically coupled Co layers in larger grain size because the spin-dependent scattering of electrons with a long mean free path becomes more effective than that of electron scattering from grain boundaries.[30]

Magnetic characterizations.— As an example, the magnetization curves of the CoNiCu/Cu multilayer deposited from the electrolyte with 0.02 M Ni concentration are given in Fig. 11. The magnetic field was applied parallel and perpendicular to the film plane. The

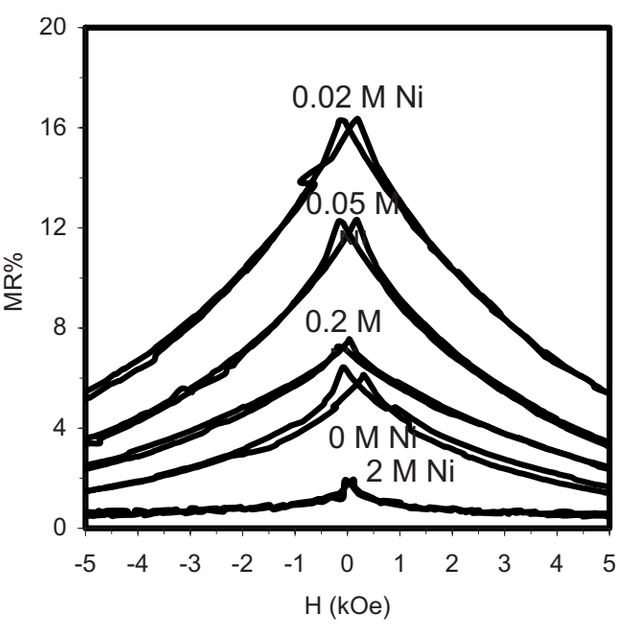

Figure 9. TMR peaks of 426[CoNiCu (4 nm)/Cu (0.7 nm)] multilayers depending on the Ni concentration in the electrolyte at low applied field (5 kOe).

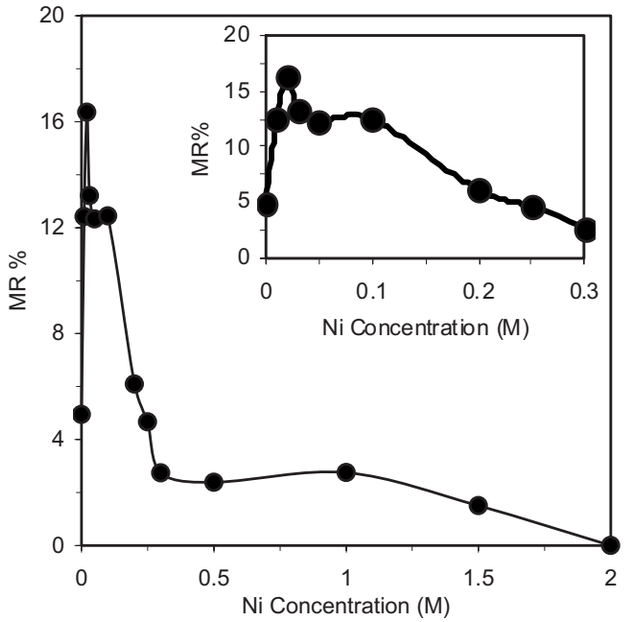

Figure 10. Variation in GMR in CoNiCu/Cu multilayers with the Ni concentration in the electrolyte.

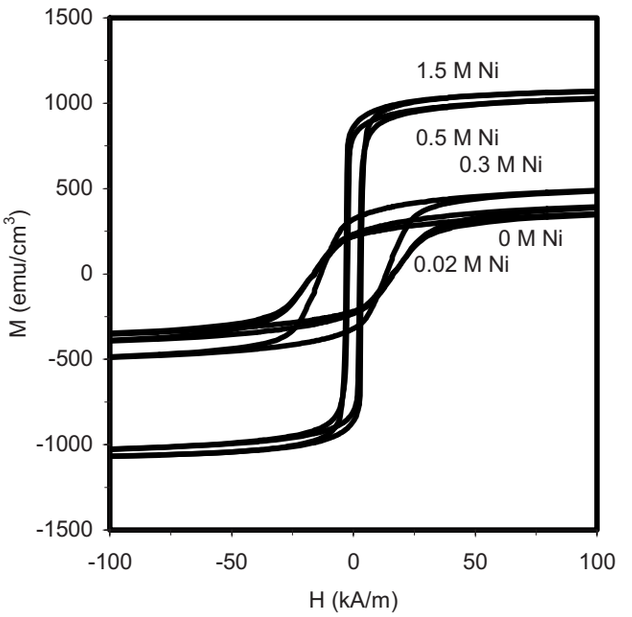

Figure 12. The evolution of hysteresis curves of CoNiCu/Cu multilayers according to Ni concentration in the electrolyte.

solid lines show the hysteresis loop in the film plane and the dashed lines belong to the one that are perpendicular to the film plane. As seen from the figure, the saturation field in the film plane is smaller than that in the perpendicular one. This indicates that the easy axis of the sample is in the film plane. Similar results were obtained for all samples. Figure 12 displays the evolution of the hysteresis curves in the film plane for the CoCu/Cu and CoNiCu/Cu multilayers with different Ni concentrations. As expected, the magnetic moment per volume increases due to the increase in the Ni content in the electrolyte and hence in the samples. Also, for CoCu/Cu and CoNiCu/Cu multilayers grown from electrolytes containing Ni concentration up to 0.3 M, the hysteresis shapes are sigmoid. For CoNiCu/Cu multilayers deposited from the electrolytes containing more than 0.3 M Ni, rectangular hysteresis loops are obtained. The sigmoidal shape of the magnetization curves arises from superparamagnetic (SPM) regions. The rectangular magnetization curves reflect that as the Ni content of the film increases, the SPM regions get smaller and the ferromagnetic interactions begin to be more effective.[31]

The change in the remanent (M_r) and saturation (M_S) magnetizations with the Ni concentration is shown in Fig. 13. An increase in M_r values depending on Ni concentration in the electrolyte indicates that ferromagnetic interactions are stronger for the CoNiCu/Cu multilayers produced from the electrolytes with high Ni concentrations.

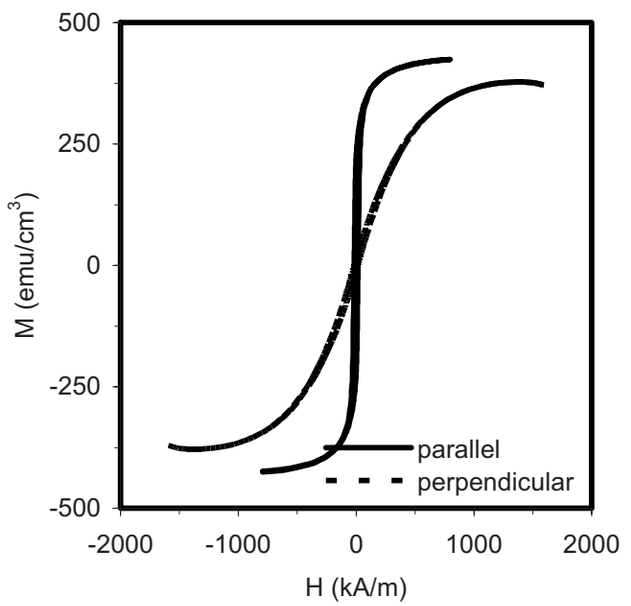

Figure 11. Hysteresis curves of CoNiCu/Cu multilayer grown from the electrolyte containing 0.02 M Ni.

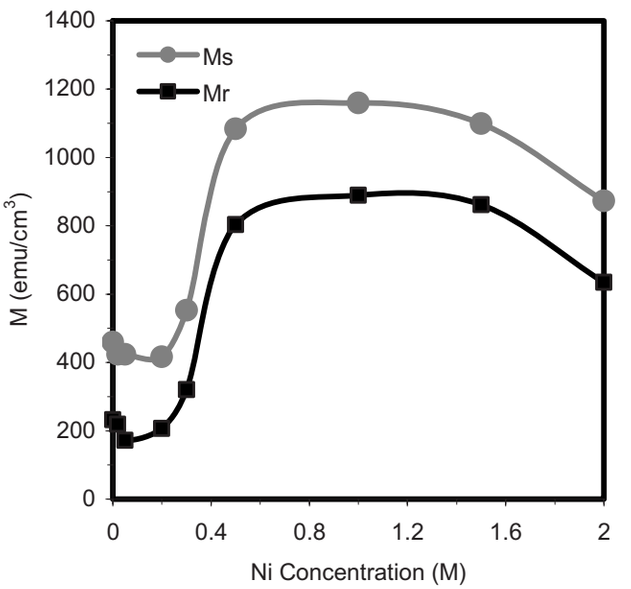

Figure 13. Remanent magnetization (M_r) and saturation magnetization (M_S) values of the CoNiCu/Cu multilayers as a function of the Ni concentration in the electrolyte.

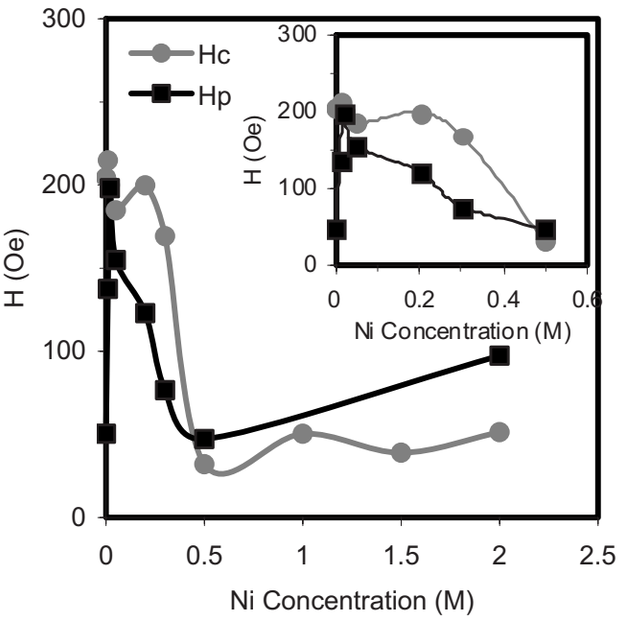

Figure 14. Variation in the peak field (H_p) and the coercivity field (H_C) due to Ni concentration in the electrolyte.

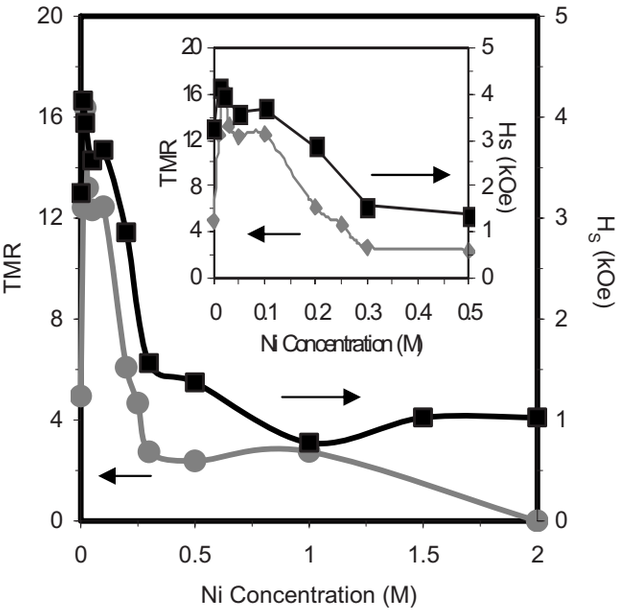

Figure 15. Change in the saturation field and the TMR values of CoNiCu/Cu multilayers as a function of Ni concentration in the electrolyte.

In these samples, the appearance of AMR at low fields also confirms the strong ferromagnetic interaction. The M_S values of the multilayers are smaller than that of bulk Co (1420 emu/cm^3) due to the finite size effect.[32] As seen from Fig. 13, the M_S values increase as the Ni concentration increases. This is probably due to the increase in Co atoms having a high magnetic moment in the ferromagnetic layer because Ni addition into the electrolytes based on cobalt sulfate prevents the dissolution of Co occurring during the deposition of Cu. The decrease in the saturation magnetization of the CoNiCu/Cu multilayers grown from the electrolytes with 2.0 M Ni may be attributed to the dead area of magnetization at the interfaces between CoNi and Cu layers.[33,34] The remanence ratio M_r/M_S was $\sim$0.4 for the samples grown from the electrolytes with Ni ion concentrations below 0.1 M, $\sim$0.6 for Ni concentrations between 0.1 and 1.0 M, and $\sim$0.7 for Ni concentrations of over 1.0 M. This suggests that the antiferromagnetic coupling between NiCo layers weakens as the Ni concentration in the electrolyte and hence the Ni content of the film increase.

Figure 14 demonstrates the change in the coercive field (H_C) and the MR peak field (H_P) of CoNiCu/Cu multilayers with the Ni concentration in the electrolyte. Furthermore, the inset in the figure shows the variation in H_C (gray circles) and H_P (black squares) for Ni concentrations below 0.5 M. The coercive field values are larger than that of bulk Co (20 Oe) due to finite size effect. As seen from the figure, both H_C and H_P values rise up to 0.02 M Ni concentration and beyond this point both of them continuously decrease. For Ni concentrations more than 0.5 M, H_C becomes almost constant and H_P slightly increases. Because H_P is defined as the field of the maximum antiparallel alignment in adjacent ferromagnetic layers and H_C is the magnetic field to require vanishing magnetization, there is a small difference between H_C and H_P. The decrease in the coercive field with increasing Ni content was also observed in a previous work. It was reported that the Ni content enhanced the sensitivity of the multilayers.[35]

The saturation field (H_S) and TMR values of CoNiCu/Cu multilayers as a function of the Ni concentration in the electrolyte are illustrated in Fig. 15. In the inset of Fig. 15, H_S and TMR values are drawn in detail for Ni concentrations below 0.5 M. H_S reflects the strength of the antiferromagnetic interlayer exchange coupling (J_i) according to Eq. 3 and hence the GMR value. As seen from Fig. 15, the H_S and TMR vary almost coherently. For low Ni concentrations, large H_S values are a result of the presence of SPM regions.[36]

Conclusions

A series of CoNiCu/Cu multilayers was grown on strong (100) textured Cu substrates from electrolytes containing different Ni ion concentrations. XRD patterns showed that all studied samples exhibited an fcc structure with different preferred orientations. It was observed that most of multilayers have the same texture as in their substrate (100), but few samples indicated a weak (111) orientation. This suggests that the Cu substrate induces the growth of the multilayers in the (100) direction. As expected, because the Ni content of the film increase as the Ni concentration in the electrolyte is increased, the lattice parameter approaches that of the bulk Ni. For CoNiCu/Cu multilayers grown from the electrolyte containing Ni up to 0.2 M, the GMR magnitude is larger than that of CoCu/Cu multilayers and its maximum value was observed for the samples deposited from the electrolyte with 0.02 M Ni. This is an indication that Ni improves the multilayer structure. For the samples prepared from the electrolyte including Ni more than 1.5 M, the AMR was predominantly observed. The decreases in GMR with more Ni addition into the ferromagnetic layers is based on the fact that the antiferromagnetic coupling between the Ni layers is weaker compared with that in the Co layers. In addition, as the Ni addition is increased, although the Cu content decreases, the decreases in the GMR arise from the fact that the electrolyte pH plays a more effective role on the GMR of electrodeposited NiCoCu/Cu multilayers. The hysteresis loops by VSM revealed that the easy axes of CoNiCu/Cu multilayers are in the film plane. The shape of hysteresis curves converted from sigmoid to rectangular as the Ni content in the electrolyte and hence in the films increases. M_S and M_r values rise with increasing Ni concentration. It was observed that the M_S values for all multilayers are smaller than that of bulk Co, attributed to the finite size effect. Furthermore, H_C values decrease with addition of Ni.

Acknowledgments

This work was supported by the Scientific and Technical Research Council of Turkey (TUBITAK) under grant no TBAG-1771,

Balıkesir University Research under grant no 2005/18, and The State Planning Organization (DPT) under grant no 2005K120170. Anadolu University, Materials Science and Engineering Department is gratefully acknowledged for the SEM and EDX measurements.

University of Uludag assisted in meeting the publication costs of this article.

References

1. F. Figueiras, E. Rauwel, V. S. Amaral, N. Vyshatko, A. L. Kholkin, C. Soyer, D. Remiens, V. V. Shvartsman, P. Borisov, and W. Kleemann, *J. Vac. Sci. Technol. A*, **28**, 6 (2010).
2. H. Chihaya, M. Kamiko, and R. Yamamoto, *Thin Solid Films*, **515**, 2542 (2006).
3. L. Tong, J. Du, M. Pan, M. Lu, D. Feng, L. Chen, X. Jin, and H. Zhai, *J. Magn. Magn. Mater.*, **198–199**, 273 (1999).
4. J. Zhang, M. Moldovan, D. P. Young, and J. Podlaha, *J. Electrochem. Soc.*, **152**, C626 (2005).
5. L. Peter, J. Padar, E. Toth-Kadar, A. Cziraki, P. Soki, L. Pogany, and I. Bakonyi, *Electrochim. Acta*, **52**, 3813 (2007).
6. S. M. S. I. Dulal, E. A. Charles, and S. Roy, *Electrochim. Acta*, **49**, 2041 (2004).
7. O. I. Kasyutich, W. Schwarzacher, V. M. Fedosyuk, P. A. Laskarzhevskiy, and A. I. Masliy, *J. Electrochem. Soc.*, **147**, 2964 (2000).
8. V. Weihnacht, L. Peter, J. Toth, J. Padar, Zs. Kerner, C. M. Schneider, and I. Bakonyi, *J. Electrochem. Soc.*, **150**, C507 (2003).
9. J. J. Kelly, P. E. Bradley, and D. Landolt, *J. Electrochem. Soc.*, **147**, 2975 (2000).
10. K. Hong, J. Lee, J. Lee, Y. D. Ko, J. S. Chung, and J. G. Kim, *J. Magn. Magn. Mater.*, **304**, 60 (2006).
11. M. Alper, W. Schwarzacher, and S. J. Lane, *J. Electrochem. Soc.*, **144**, 2346 (1997).
12. G. Nabiyouni, W. Schwarzacher, Z. Rolik, and I. Bakonyi, *J. Magn. Magn. Mater.*, **253**, 77 (2002).
13. B. D. Cullity, *Elements of X-Ray Diffraction*, 2nd ed., p. 141, Addison-Wesley, London (1978).
14. A. Vicenzo and P. L. Cavalotti, *Electrochim. Acta*, **49**, 4079 (2004).
15. D. Rafaja, H. Fuess, D. Simek, L. Zdeborova, and V. Valvoda, *J. Phys.: Condens. Matter*, **14**, 10021 (2002).
16. Y. S. Gu, W. P. Chai, Z. H. Mia, J. G. Zhao, M. Li, L. M. Mei, C. Dong, F. Wu, and H. Chen, *Phys. Rev. B*, **50**, 6119 (1994).
17. I. Bakonyi, E. Simon, B. G. Toth, L. Peter, and L. F. Kiss, *Phys. Rev. B*, **79**, 174421 (2009).
18. N. Zech, E. J. Podlaha, and D. Landolth, *J. Electrochem. Soc.*, **146**, 2886 (1999).
19. J. Gong, W. H. Butler, and G. Zangari, *Appl. Phys. Lett.*, **87**, 012505 (2005).
20. S. M. S. I. Dulal and E. A. Charles, *J. Alloys Compd.*, **455**, 274 (2008).
21. T. R. McGuire and R. I. Potter, *IEEE Trans. Magn.*, **11**, 1018 (1975).
22. S. Z. Hua, D. S. Lashmore, L. Salamanca-Riba, W. Schwarzacher, L. J. Swartzenruber, R. D. McMichael, L. H. Bennett, and R. Hart, *J. Appl. Phys.*, **76**, 6519 (1994).
23. S. Z. Hua, L. Salamanca-Riba, L. H. Bennett, L. J. Swartzendruber, R. D. McMichael, D. S. Lashmore, and M. Schlesinger, *Scr. Metall. Mater.*, **33**, 1643 (1995).
24. M. Alper, M. C. Baykul, L. Peter, J. Toth, and I. Bakonyi, *J. Appl. Electrochem.*, **34**, 841 (2004).
25. H. Kubota, M. Sato, and T. Miyazaki, *J. Magn. Magn. Mater.*, **167**, 12 (1997).
26. K. D. Bird and M. Schlesinger, *J. Electrochem. Soc.*, **142**, L65 (1995).
27. A. Paul, T. Damm, D. E. Bürgler, S. Stein, H. Kohlstedt, and P. Grünberg, *J. Phys.: Condens. Matter*, **15**, 2471 (2003).
28. X. Bian, B. D. Gaulin, J. O. Ström-Olsen, Z. Altounian, C. V. Stager, and J. A. Avelar, *Phys. Rev. B*, **50**, 3114 (1994).
29. A. Fert, A. Barthelemy, P. Etienne, S. Lequien, R. Loloee, D. K. Lottis, D. H. Mosca, F. Petroff, W. P. Pratt, and P. A. Schroeder, *J. Magn. Magn. Mater.*, **104–107**, 1712 (1992).
30. A. R. Modak, D. J. Smith, and S. S. P. Parkin, *Phys. Rev. B*, **50**, 4232 (1994).
31. S. K. Ghosh, A. K. Grover, P. Chowdhury, S. K. Gupta, G. Ravikumar, D. K. Aswal, M. Senthil Kumar, and R. O. Dusane, *Appl. Phys. Lett.*, **89**, 132507 (2006).
32. M. Prutton, *Thin Ferromagnetic Films*, Butterwords, London (1964).
33. I. Bakonyi, J. Toth, L. F. Kiss, E. Toth-Kadar, L. Peter, and A. Dinia, *J. Magn. Magn. Mater.*, **269**, 156 (2004).
34. D. Miyauchi and S. Araki, *Jpn. J. Appl. Phys., Part 2*, **34**, L31 (1995).
35. X. Bian, J. O. Ström-Olsen, Z. Altounian, Y. Huai, and R. W. Cochrane, *J. Appl. Phys.*, **75**, 7064 (1994).
36. D. K. Pandya, P. Gupta, S. C. Kashyap, and S. Chaudhary, *J. Magn. Magn. Mater.*, **321**, 974 (2009).